Biophysical Journal, Volume *111*

Supplemental Information

Intact Telopeptides Enhance Interactions between Collagens

Marjan Shayegan, Tuba Altindal, Evan Kiefl, and Nancy R. Forde

Table of Contents

Chemical equilibrium parameters

For telopeptide-dependent association between collagens, parameters for K_{eq} were based on an estimate provided by Prockop and Fertala (1). There they estimated the binding constant between the α1 C-terminal telopeptide and a neighboring triple helix to be K_d = 5 μM. Specific association of a similar order of magnitude was found in other peptide-collagen experiments (2, 3). Because telo-collagen contains many possible interacting domains, we assumed a stronger interaction between chains, of $K_{eq,telo} = 5\times10^6$ M^{-1} (corresponding to a K_d = 0.2 μM). For the pepsin-treated "atelo-collagen" sample, telopeptides are incompletely removed (4, 5). In this case, we assumed that some association between collagens remained, but the removal of much of each telopeptide would result in a weaker overall binding. For "atelo-collagen" we thus took $K_{eq,atelo} = 5\times10^5$ M^{-1}. The concentration of each species was determined for each total collagen concentration according to equation (6) in the main text. These respective values gave rise to the concentration-dependent population of unimers, dimers, trimers etc. shown in Figure S1.

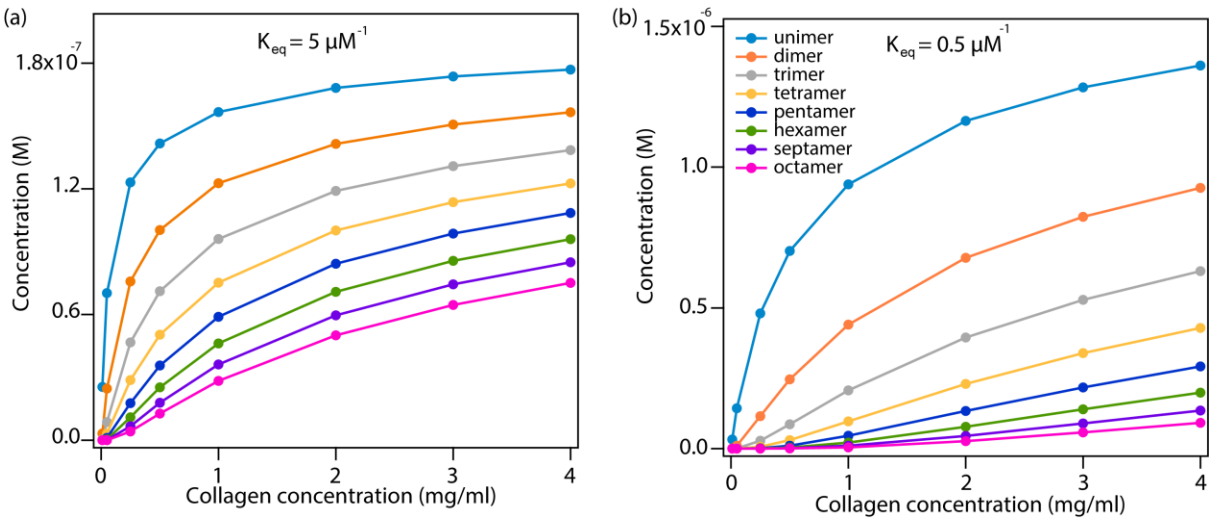

Figure S1. Chemical equilibrium predictions of concentration-dependent multimers of collagen. Molar concentration of each species calculated for (a) $K_{eq,telo}$ = 5 μM^{-1} and (b) $K_{eq,atelo}$ = 0.5 μM^{-1}. Only the first eight species are shown.

Rouse model parameters

Model parameters used in the Rouse polymer model are provided in Table S1.

In treating collagen as a Rouse chain, we are assuming it to be flexible. Parameter values for its persistence length l_p range widely (6–9); for its treatment as a Rouse chain we are considering one of the shortest values from the literature of 15 nm (6), which corresponds to a Kuhn length of b=30 nm. While a collagen unimer has only 10 Kuhn segments, the approximation of flexible polymers becomes increasingly good with longer multimers.

To obtain the drag coefficient for each segment, ζ, we approximated each Kuhn segment as a slender body of length l=30 nm and a radius of r=0.75 nm. Taking the dynamic viscosity of water μ=0.978 mPa·s at 21°C, the drag coefficients along the axis of the Kuhn segment and perpendicular to it were calculated to be $\zeta_{\parallel} = 2\pi\mu l / (\ln(l/r)) = 0.5\times10^{-10}$ N·s/m and $\zeta_{\perp} = 4\pi\mu l / (\ln(l/r)) = 1\times10^{-10}$ N·s/m, respectively. A similar value for ζ was determined by approximating collagen as a sphere with radius of gyration $R_g = \sqrt{l_p L/3} = 39$ nm (10). The drag coefficient of the sphere was calculated using the Stokes equation, then divided by 10 - the number of Kuhn segments in a collagen molecule - which yielded $\zeta = 2\pi\mu R_g / 10 = 0.7\times10^{-10}$ N·s/m. The translational diffusion constant measured for collagen in DLS experiments, D_t = 8.4×10^{-12} m^2/s (see Figure S4), also indicates $\zeta = (k_B T / D_t)/10 = 0.5\times10^{-10}$ N·s/m. We assumed a typical value of $\zeta = 0.5\times10^{-10}$ N·s/m in our calculations.

For isotropically distributed collagen unimers in solution, the average distance between centers of mass decreases from d=125-50 nm as concentration increases from 0.25-4 mg/ml. The calculated average diameter of $2R_g$=78 nm for collagen results in good agreement with overlap concentrations c* of ~1 mg/ml (11, 12).

Supplementary Table S1. Parameter values used for modelling Rouse chains.

Parameter	Description	Value
T	Temperature	294 K
L	Contour length of collagen	300 nm
b	Kuhn segment length	30 nm
a_0	Density parameter	0.7
ζ	Segmental drag coefficient	0.5×10^{-10} N.s/m

Collagen purity

We discuss the possibility that impurities in the commercially-sourced collagen contribute to the differences we measure between telo and atelo collagen. Coommassie staining of denatured collagen separated by SDS-PAGE shows that commercial samples of both telo- and atelo-collagen contain some degradation products or other protein contaminants (Figure S2a). Given their size, small protein contaminants are not expected to add low-frequency modes to the sample's shear modulus, and the independence of moduli on bead size and surface chemistry discount interactions with the probe particles as contributing to the measured moduli (13). Furthermore, treatment with pepsin does not result in a disappearance of possible contaminant bands, meaning that they are present in both telo- and atelo-collagen.

Examination of stock telo-collagen by a more sensitive fluorescence imaging technique implies high purity collagen (Figure S2b). For this experiment, lysine residues in telo-collagen from two different commercial stocks were fluorescently labeled at pH 9.3, following a protocol from references (13, 14). No purification of the collagen was performed prior to gel electrophoresis. When these samples were imaged either via fluorescence or silver-staining, they appeared highly pure. The difference observed in SDS-PAGE in apparent purity between collagen samples originating in acidic (Fig. S2a) versus alkaline (Fig. S2b) pH may arise from acid-induced hydrolysis of collagen occurring at the elevated temperatures used for sample denaturation (95°C in our experiments) (15).

Based on this analysis, the predominant difference between telo- and atelo-collagen samples appears to be the proteolytic removal of telopeptides by pepsin.

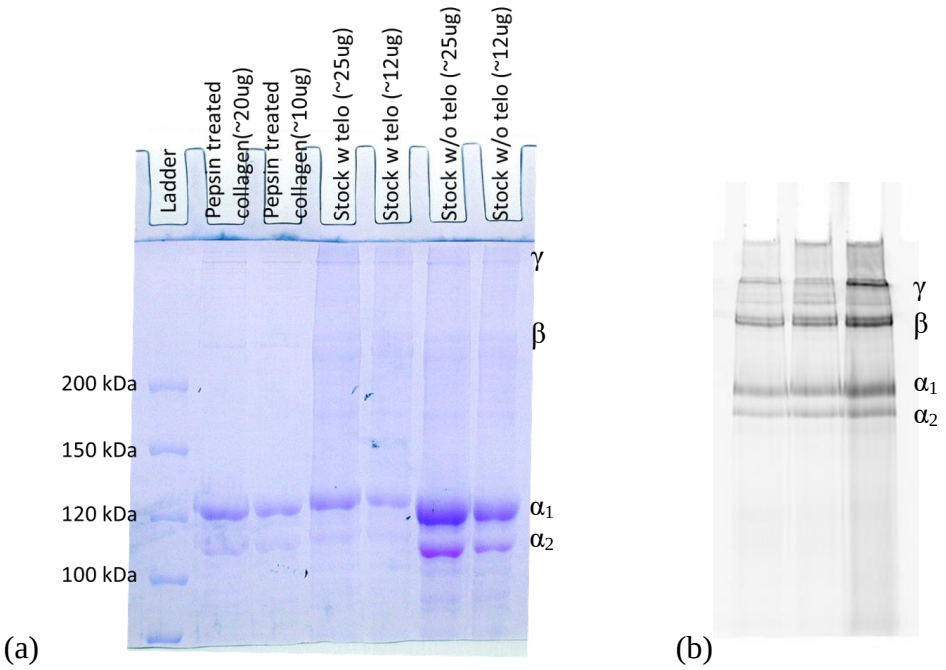

Figure S2. SDS-PAGE analysis of collagen and its pepsin cleavage products. α_1 and α_2 refer to the two component chains of the $(\alpha_1)_2(\alpha_2)_1$ type I collagen triple helix. β and γ bands denote two and three, respectively, crosslinked α-chains. These are a standard feature seen in SDS-PAGE gels of collagen and predominantly arise from crosslinking between chains within a triple helix. (Other bands of high molecular weight that might correspond to permanent intermolecular crosslinks between triple helices exhibit very weak intensity.) (a) The shortening of pepsin-treated collagen relative to stock control (telo) sample results in a small but discernable increase in electrophoretic mobility. All samples exhibit a similar small extent of bands that do not correspond to full-length collagen, retained following pepsin treatment. (b) Fluorescence image of an SDS-PAGE gel containing fluorescently labeled collagen samples. Here, the left lane contains the telo-collagen stock solution used in this paper (Invitrogen) and the other two lanes contain rat type I telo-collagen from a different supplier (Sigma, C7661). This imaging technique and preparation from alkaline buffer indicates a high purity of telo-collagen.

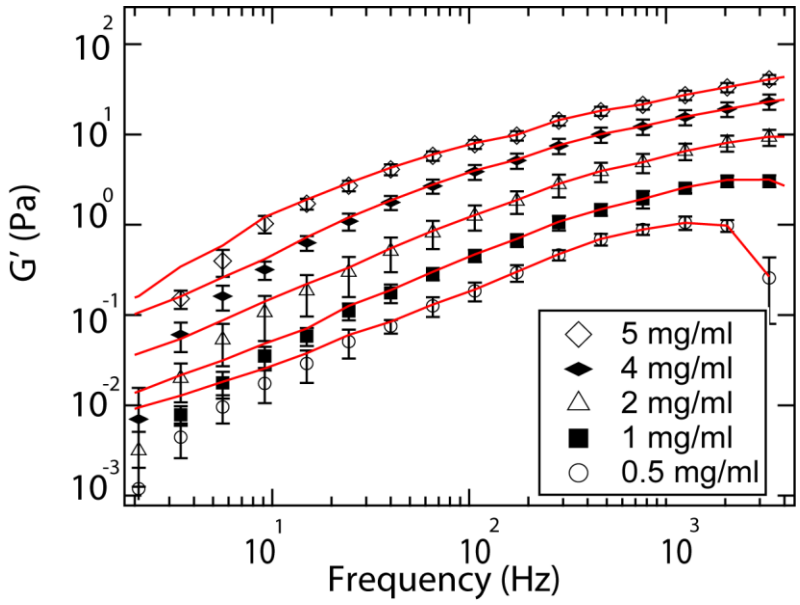

Figure S3. Two methods of correcting the measured elasticity (not shown) for trap modulus give statistically indistinguishable results for $G'(f)_{sample}$ above 10 Hz. Red lines assume G'_{trap} is represented by the lowest-frequency value of $G'(f)_{measured}$, which is subtracted from all other $G'(f)_{measured}$ values to obtain $G'(f)_{sample}$. Symbols assume G'_{trap} is represented by an average of the lowest five $G'(f)_{measured}$ values, which is subtracted from all $G'(f)_{measured}$ values to obtain $G'(f)_{sample}$.

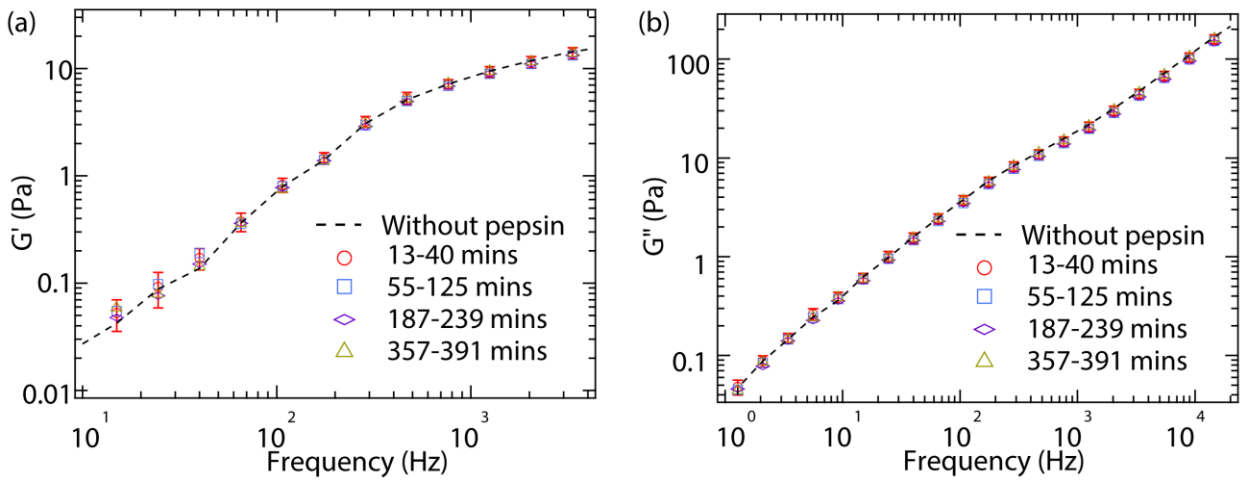

Figure S4. Incubation of atelo collagen with pepsin leads to no time-dependent change in either (a) elastic or (b) viscous modulus. Incubation conditions of 2 mg/ml collagen and 0.5 μg/ml pepsin are as in Figure 4, where a significant decrease in both *G'* and *G"* was observed when telo-collagen was incubated with pepsin. Symbols represent means of moduli from five independent measurements in each stated time interval, and error bars represent the standard errors of the mean.

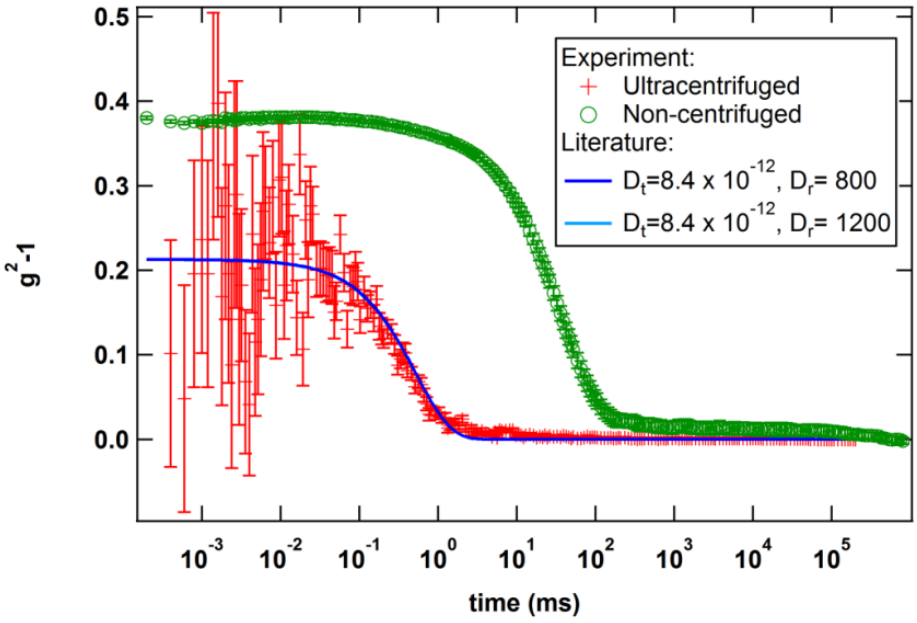

Figure S5. Ultracentrifugation removes large aggregates of collagen. Commercial atelo-collagen (green circles) contains large structures, as indicated by the long decorrelation times in dynamic light scattering signal. Following ultracentrifugation, the dynamic light scattering response of the unsedimented sample corresponds well to single collagen chains, as previously described in the literature with translational and rotational diffusion constants presented in the inset (units of m^2/s and s^{-1}, respectively) (7). The two predictions are indistinguishable at this detection angle (45°).

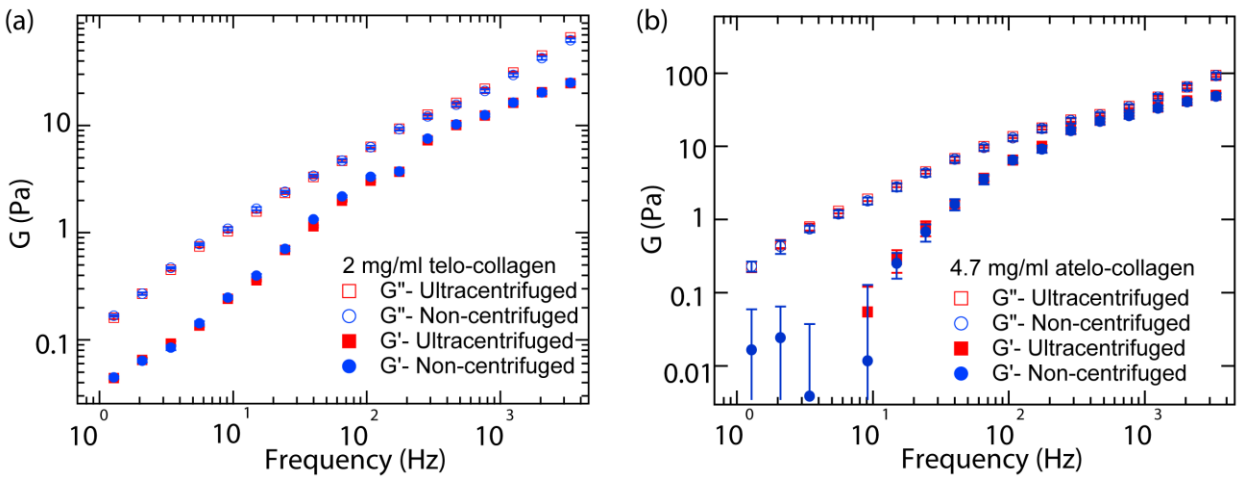

Figure S6. Treatment of the collagen solutions by ultracentrifugation does not significantly impact the microrheology results for (a) telo-collagen (2 mg/ml) or (b) atelo-collagen (4.7 mg/ml). As discussed in the text, this likely arises from the selection of traces for analysis with this technique, which eliminate any involving significant disruption of the mean position of the trapped particle from equilibrium.

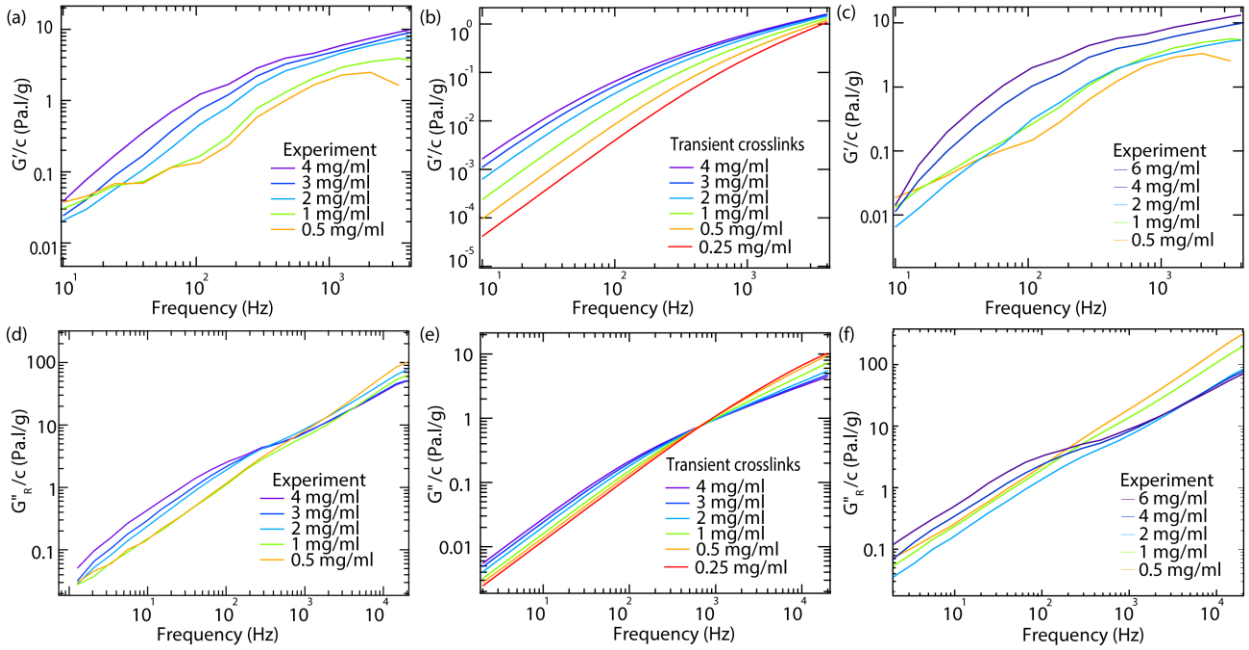

Figure S7. Comparison of the frequency-dependent behavior of G'/c and G_R''/c for atelo-collagen over a wide range of collagen concentrations c, and comparison with model predictions. Experimental results for in-house prepared atelo-collagen are shown in (a) and (d); model predictions assuming transient crosslinks with $K_{eq,atelo} = 0.5\ \mu M^{-1}$ are presented in (b) and (e); commercially obtained atelo-collagen experimental results are shown in (c) and (f).

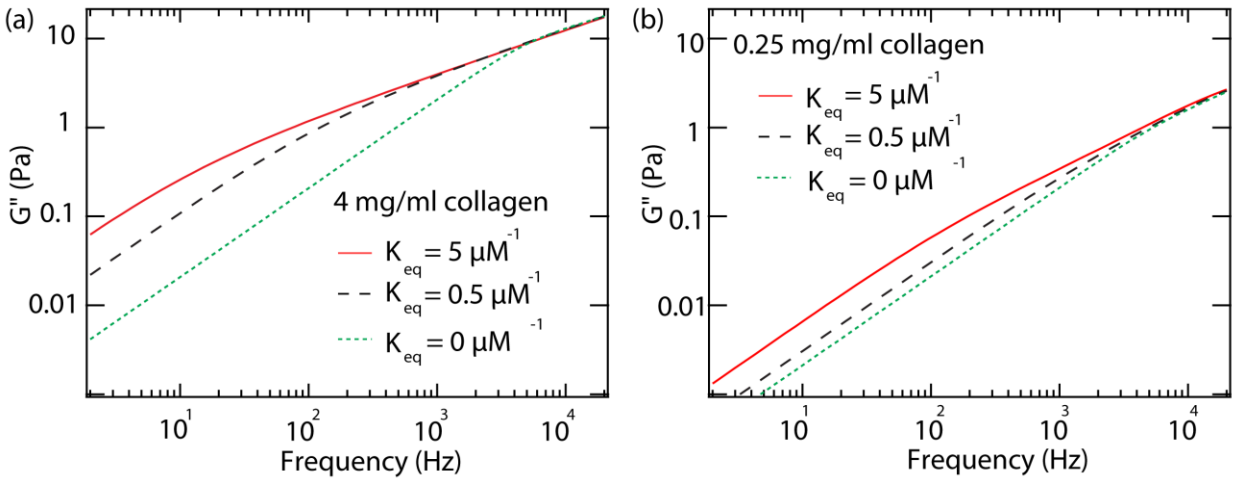

Figure S8. Restricted Rouse model predictions comparing the viscous moduli of unimer-only collagen (e.g. completely lacking telopeptides) with associating telo- and atelo-collagen chains. The latter data are reproduced from Figure 8 in the text. (a) 4 mg/ml; (b) 0.25 mg/ml.

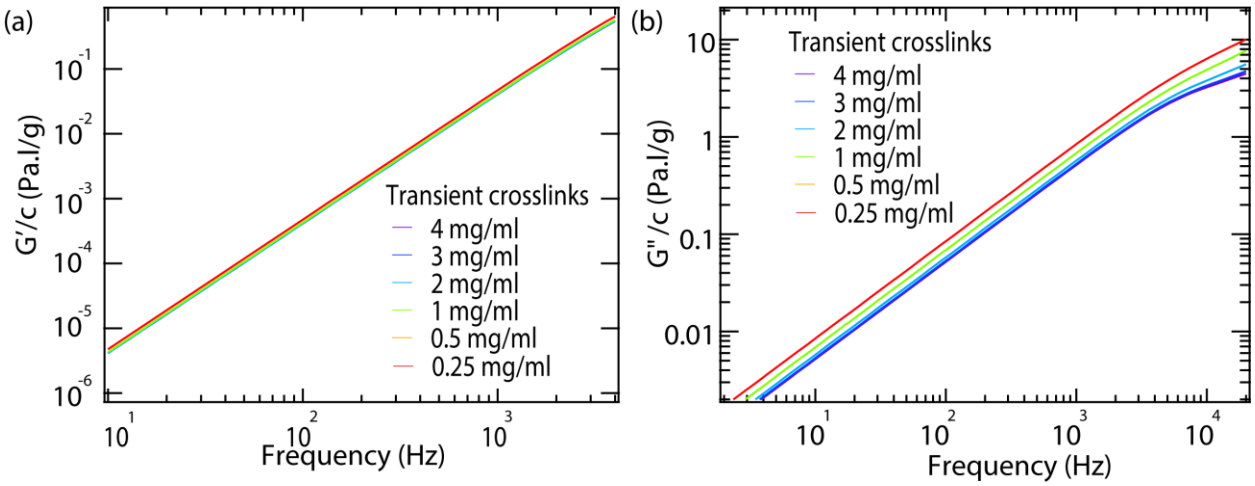

Figure S9. Restricted Rouse model predictions for the case of non-associating polymers (K_{eq}=0), such as would be predicted for collagen completely lacking telopeptides. In the experimentally accessible frequency range, *G'* is predicted to scale linearly with concentration. *G"* is predicted to increase sublinearly with concentration. Note the substantially smaller low-frequency elastic modulus here compared with solutions containing multimers (Fig. 9), which results from the lack of long-range modes in this unimer-only system.

Supporting references

1. Prockop, D.J., and A. Fertala. 1998. Inhibition of the self-assembly of collagen I into fibrils with synthetic peptides. Demonstration that assembly is driven by specific binding sites on the monomers. J. Biol. Chem. 273: 15598–15604.
2. Helseth, D.L., and A. Veis. 1981. Collagen Self-Assembly Invitro - Differentiating Specific Telopeptide-Dependent Interactions Using Selective Enzyme Modification and the Addition of Free Amino Telopeptide. J. Biol. Chem. 256: 7118–7128.
3. Bhatnagar, R.S., J.J. Qian, and C.A. Gough. 1997. The role in cell binding of a beta-bend within the triple helical region in collagen alpha 1 (I) chain: structural and biological evidence for conformational tautomerism on fiber surface. J. Biomol. Struct. Dyn. 14: 547–60.
4. Hulmes, D.J.. 2008. Collagen. Boston, MA: Springer US.
5. Drake, M.P., P.F. Davison, S. Bump, and F.O. Schmitt. 1966. Action of Proteolytic Enzymes on Tropocollagen and Insoluble Collagen. Biochemistry. 5: 301–312.
6. Sun, Y.-L., Z.-P. Luo, A. Fertala, and K.-N. An. 2002. Direct quantification of the flexibility of type I collagen monomer. Biochem. Biophys. Res. Commun. 295: 382–386.
7. Claire, K., and R. Pecora. 1997. Translational and Rotational Dynamics of Collagen in Dilute Solution. J. Phys. Chem. B. 101: 746–753.
8. Lovelady, H.H., S. Shashidhara, and W.G. Matthews. 2014. Solvent specific persistence length of molecular type I collagen. Biopolymers. 101: 329–335.
9. Varma, J., S. Orgel, and J. Schieber. 2016. Nanomechanics of Type I Collagen. Biophys. J. 111: pp: 50–6.
10. Teraoka, I. 2002. Polymer Solutions: An Introduction to Physical Properties. New York: John Wiley & Sons.
11. Shayegan, M., and N.R. Forde. 2013. Microrheological Characterization of Collagen Systems: From Molecular Solutions to Fibrillar Gels. PLoS One. 8: e70590.
12. Oechsle, A.M., X. Wittmann, M. Gibis, R. Kohlus, and J. Weiss. 2014. Collagen entanglement influenced by the addition of acids. Eur. Polym. J. 58: 144–156.
13. Shayegan, M. 2014. Determining local viscoelastic properties of collagen systems using optical tweezers. Ph.D. Dissertation, Simon Fraser University.
14. Han, S., D.J. McBride, W. Losert, and S. Leikin. 2008. Segregation of type I collagen homo- and heterotrimers in fibrils. J. Mol. Biol. 383: 122–32.
15. Cannon-Carlson, S., and J. Tang. 1997. Modification of the Laemmli Sodium Dodecyl Sulfate–Polyacrylamide Gel Electrophoresis Procedure to Eliminate Artifacts on Reducing and Nonreducing Gels. Anal. Biochem. 246: 146–148.